Moreover, the decrease of the transition temperature of alkyl-substituted polythiophenes to a less conjugated state with increasing length of the side chains[26] has been asigned to a similar deviation from planarity. Apparently, the steric hindrance of a substituent at the 3-positions of polypyrrole or polythiophene is not negligible.

One of the aspects of self-doped polypyrroles not yet fully understood is the dependence of properties on the way of preparation. All electrochemical variables such as voltage, current density, conduction salt, solvent, electrode material, and type of cell influence the morphology, conductivity, and solubility of the polymers. This dependence is best reflected in the NMR spectra of the aqueous solutions of the self-doped polypyrroles. ^{1}H NMR data of the polymers in D_2O confirm the charged backbones. However, although the H atom attached directly to the pyrrole ring is found as a broad peak shifted downfield by about 1 ppm, its intensity is always too low and sometimes even vanishingly small. Since no clear differences are observed in the electronic spectra and, hence, in the level of doping, a more detailed study of this dependence will be necessary.

Conclusions

3-Substituted pyrroles are made by a three-step synthesis from *N*-(phenylsulfonyl)pyrrole. A tedious purification of the sodium salts of these monomers for self-doped polypyrroles has been adopted. The low oxidation potential of these monomers allows a direct oxidative electrochemical polymerization. The possibility of performing this polymerization without the addition of another conduction salt is a direct proof of the self-doped state of the polymer formed. The polymers **15** and **16** formed on Pt or ITO glass electrodes show neat cyclic voltammograms when these polymers are in contact with acetonitrile solutions containing protons. On the other hand, polymer **17** shows only a minor electrochemical response. From elemental analyses it is clear that the polymers contain an excess of oxygen, partly as water. X-ray analysis shows that the polymers are amorphous. ESR data show that only one spin per 150–300 rings is present, and the charge carriers are mainly bipolarons. From UV–vis–NIR spectra it is clear that the doping level is comparable to plain polypyrrole but that the polarons must have different configurations. This is ascribed to less planar conjugated chains in the substituted polypyrroles. The polymers are sparingly soluble in water. UV–vis–NIR spectra of such stable solutions indicate that the chains remain largely self-doped. The conductivity of the polymers ranges from 10^{-3} to 0.5 S/cm. The low values may partly be due to the deviations from planarity of the conjugated backbones. Since the self-doped polymers are water soluble, it is possible to record ^{1}H NMR spectra of aqueous solutions. This makes research to the molecular origin of conductivity in polymers feasible.

Acknowledgment. Thanks are due to L. W. van Horssen and I. Rotte (Philips Research) for their assistance during many of the experiments and to W. H. Kruizinga (University of Groningen) for recording the high-field ^{1}H NMR spectra. The analytical departments of both laboratories are gratefully acknowledged.

(26) Ingenäs, O.; Gustafsson, G.; Saleneck, W. R.; Österholm, J. E.; Laakso, J. *Synth. Met.* **1989**, *28*, C377.

Influence of Oxygen Partial Pressure on the Synthesis of $Ba_2YCu_3O_7$ from a Novel Oxalate Precursor

P. K. Gallagher* and D. A. Fleming

AT&T Bell Laboratories, Murray Hill, New Jersey 07974

Received July 11, 1989

An oxalate precursor precipitate is prepared by reacting carbonate, hydroxide, and/or oxides with oxalic acid in a heated aqueous solution. By this approach, there are no extraneous anions or cations introduced by the starting salts or created during the reaction since the products are only water and carbon dioxide. Specific solubility differences may be compensated by recycling the filtrate. The thermal conversion of the resulting coarse crystalline precipitate to the desired oxide product is studied by thermoanalytical techniques and X-ray diffraction. The oxygen content and, hence, the defect structure of the product depend upon the partial pressure of oxygen and the temperature. Consequently, the kinetics of the final stage of the reaction, eq 1, are influenced by the value of x.

Introduction

There has been an enormous interest generated in cuprate systems having various layered structures because a number of them have exhibited confirmed superconductivity at temperatures as high as 125 K. There have been problems associated with the stability, reproducibility, fabrication, and strength of the material as well as several crucial electrical properties, e.g., the critical current (J_c), critical field (H_c), and high-frequency ac conductivity. Many of these difficulties can be associated with the phase purity, microstructure, grain boundary effects, etc. Consequently, numerous synthetic approaches have been utilized in an effort to obtain optimum properties in the final sintered ceramic or film. Besides the conventional ceramic methods, most of the more modern "chemical" approaches, e.g., sol–gel, coprecipitation, spray roasting or drying, freeze-drying, pyrolysis of organometallics, etc., have been utilized with varying degrees of success. Two of the most successful aqueous coprecipitation techniques produce a fine hydroxide–carbonate mixture[1] or more coarse crystalline oxalate precipitate.[2,3] In terms of fil-

(1) Bunker, B. C.; et al. *In Better Ceramics Through Chemistry III*; Brinker, C. J., et al., Eds.; Materials Research Society: Pittsburgh, PA, 1988; pp 373–384.

(2) Kaneko, K.; Ihara, H.; Hirabayashi, M.; Terada, N.; Senzaki, K. *Jpn. J. Appl. Phys.* **1987**, *26*, L734.

0897-4756/89/2801-0659$01.50/0

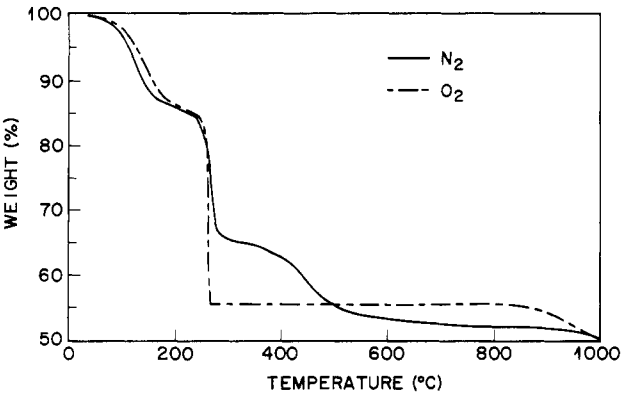

Figure 1. TG curves, $Ba_4Y_2Cu_6(C_2O_4)_{13}\cdot 20H_2O$, 10 °C min^{-1}, 95.343 mg in N_2, 83.016 mg in O_2.

terability, handling properties, and adsorbed impurities, the coarser precipitate has advantages. In this case, it also offers the possibility of greater solid solubility and, hence, more homogeneous distribution of the cations.

Oxalate coprecipitation has been used extensively in the past for many ceramic materials such as ferrites[4] and titanates.[5] In some instances such as PTC thermistors,[6] the incorporation of impurities has been used to an advantage, while in other materials[7] the incorporation of extraneous ions by occlusion, adsorption, or substitution has had deliterious effects. An approach to oxalate coprecipitation had been devised[8] to alleviate this problem by avoiding the presence of all extraneous cations and anions. This method is based on digestion of the appropriate carbonates, hydroxides, or oxides with oxalic acid. The only products of this process are the metal oxalates, water, and carbon dioxide. Added advantages are an essentially neutral solution, i.e., a pH near 7, having a very low ionic strength. These qualities in the aqueous media reduce the solubility by minimization and potential attack by excess acid or base as well as any tendency to form soluble complexes. If solubility remains a problem, it can be negated by the reuse of the filtrate after separation of the relatively coarse precipitated oxalates. This solution would be saturated with respect to the desired metallic ions and, therefore, will yield a virtually quantitative precipitate during susequent precipitation cycles. Reuse also avoids the environmental problem of waste disposal.

The coprecipitated oxalate material, which may consist of individual oxalates or solid solutions thereof, is usually converted to the intended oxide product by calcination in an atmosphere that is sufficiently oxidizing to prevent carbon residues or carbide formation.[9] Generally the only concern regarding the oxygen content of the atmosphere during calcination is that it be sufficient to prevent free carbon or metal formation by oxidation of the CO and or any metal formed from the more easily reduced oxides such as copper.[10] Most of the high-temperature superconductor systems, however, have the added factor that they have a very wide range of oxygen stoichiometry which determines their electrical and magnetic properties.

The concentration of point defects and even the crystal structure is determined by the degree of nonstoichiometry and, therefore, the partial pressure of oxygen and temperature to which the sample is exposed.[11] Previous work[2,3] on the thermal conversion of oxalate precursors to the superconducting oxide showed that the decomposition in air or oxygen below 600 °C produced an intimate mixture of $BaCO_3$, CuO, and Y_2O_3. This assemblage is better mixed and has a smaller particle size than that prepared by conventional ceramic techniques. Consequently, it reacts, see eq 1, more readily at lower temperatures to form

$$2BaCO_3 + 0.5Y_2O_3 + 3CuO \rightarrow Ba_2YCu_3O_x + 2CO_2 + \frac{6.5 - x}{2}O_2 \quad (1)$$

the desired oxide.[2,3,12] It is reasonable to expect that the solid state diffusion process in and through the product layers will influence the overall rate of reaction for this oxide formation. The rate of reaction should, therefore, be dependent upon the partial pressure of oxygen, P_{O_2}, in the atmosphere at the time.

The rate of decomposition of $BaCO_3$ has been shown to correspond with the rate of mixed oxide formation and hence, following the weight loss of the former process, is a viable means of following the rate of formation of the mixed oxide.[12] The intimately mixed and finely divided powder, resulting from the decomposition of the relatively pure oxalate formed by the process described earlier, is used as a starting material for a kinetic study based upon the P_{O_2} during the reaction. It is recognized that the naturally occurring oxygen-exchange process[11] will also affect the study by (1) superimposing an additional weight change on the measurements and (2) influencing the actual P_{O_2} of the experiment, particularly at the lowest values of P_{O_2}. It will be shown, however, that these have a relatively minor effect on the results.

Experimental Procedures and Results

Powder Preparation and Characterization. The starting materials were reagent-grade oxalic acid and barium, copper, and ytrium carbonates. The carbonates were assayed by thermogravimetry (TG) to determine their oxide equivalents. This is important due to the poorly defined amounts of carbonate, hydroxide, and water present after storage. Weighed amounts of carbonate, required to form 0.3 mol of final oxide, were placed in a beaker and mixed until the powder appeared uniform. In a separate beaker, 3 L of distilled, deionized water containing slightly more oxalic acid then that calculated for complete precipitation was heated to 60 °C and stirred magnetically on a hot plate until the acid had completely dissolved. The carbonate mixture was slowly added to the water and stirred for 48 h. The temperature of the solution was maintained at 80 °C for the first hour and then allowed to cool to room temperature. The resulting coarse crystalline precipitate was filtered by suction and rinsed with a small portion of acetone (~100 mL) prior to being air dried.

A portion of this material was calcined in O_2 at 900 °C for 30 min and the resulting powder X-rayed. Within the sensitivity of this analysis (<2 vol % crystalline impurity phases), the material was single phase. To check stoichiometry, in case of different solubilities, the filtrate from the previous precipitation was used in place of the water in the subsequent preparation. Several cycles in this manner yielded identical X-ray diffraction patterns of the calcined material, and it was concluded that, in this near neutral media without potential complexing or adsorbing ions, the precipitation was essentially quantitative.

(3) Paz-Pujalt, G. R.; Mehrotra, A. K.; Ferranti, S. A.; Agostinelli, J. A. *Solid State Ionics* **1989**, *32/33*, 1179.
(4) Gallagher, P. K.; Schrey, F. *J. Am. Ceram. Soc.* **1964**, *47*, 434.
(5) Clabaugh, W. S.; Swiggard, E. M.; Gilchrist, R. *J. Res. Natl. Bur. Std.* **1956**, *56*, 289.
(6) Gallagher, P. K.; Schrey, F.; DiMarcello, F. V. *J. Am. Ceram. Soc.* **1963**, *46*, 359.
(7) O'Bryan, H. M.; Gallagher, P. K.; Monforte, F. R.; Schrey, F. *Am. Ceram. Soc. Bull.* **1969**, *48*, 203.
(8) Gallagher, P. K.; O'Bryan, H. M.; Schrey, F.; Monforte, F. R. *Am. Ceram. Soc. Bull.* **1969**, *48*, 1053.
(9) Gallagher, P. K.; Schrey, F. *Thermochim. Acta* **1969**, *1*, 465.
(10) Dollimore, D.; Griffiths, D. L.; Nicholson, D. *J. Chem. Soc.* **1963**, 2617.
(11) Gallagher, P. K.; O'Bryan, H. M.; Sunshine, S. A.; Murphy, D. W. *Mater. Res. Bull.* **1987**, *22*, 995.
(12) Negishi, A.; Takahashi, Y.; Sakamoto, R.; Kamimoto, M.; Ozawa, T. *Thermochim. Acta* **1988**, *132*, 15.

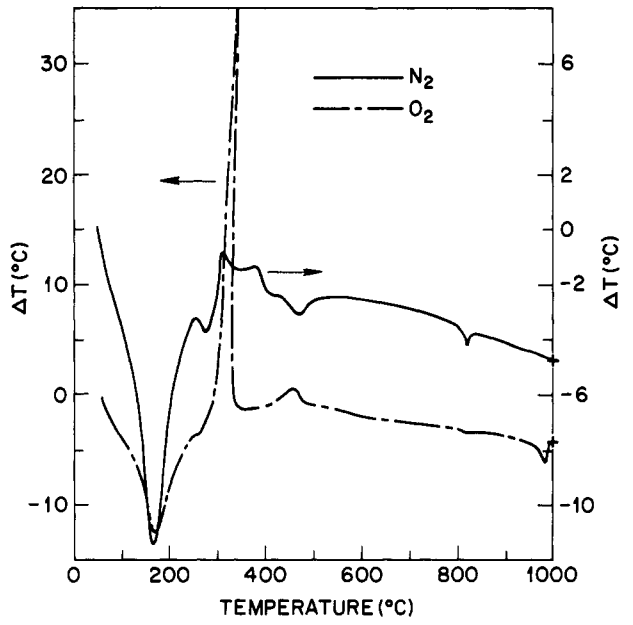

Figure 2. DTA curves, $Ba_4Y_2Cu_6(C_2O_4)_{13}\cdot 20H_2O$, 10 °C min^{-1} 61.93 mg in N_2 67.25 mg in O_2.

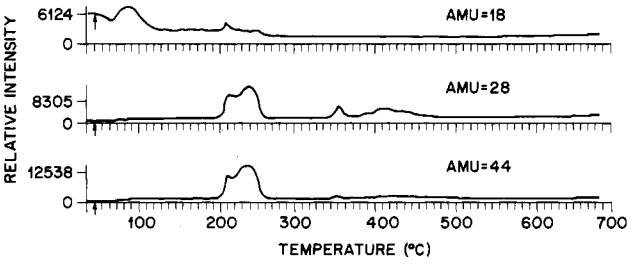

Figure 3. EGA curves, $Ba_4Y_2Cu_6(C_2O_4)\cdot 20H_2O$, 10 °C min^{-1}, vacuum 8.90 mg.

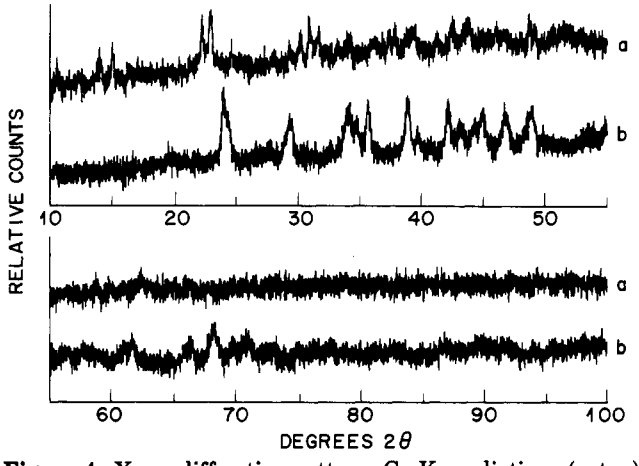

Figure 4. X-ray diffraction patterns Cu Kα radiation. (a, top) $Ba_4Y_2Cu_6(C_2O_4)_{13}\cdot 20H_2O$. (b, bottom) After calcining at 700 °C in O_2 for 30 min.

The air-dried oxalate was characterized by thermal analysis to determine the general nature of the decomposition. A Perkin-Elmer System 7 TG and DTA, Model 1700, were used. The samples were heated at 10 °C min^{-1} in an atmosphere of oxygen or nitrogen. The results are presented in Figures 1 and 2. A mass spectrometer was used to provide the evolved gas analysis (EGA) in a vacuum of $\sim 1 \times 10^{-7}$ Torr in the absence of outgassing.[13,14] Evaluation profiles for selected mass numbers are shown in Figure 3.

(13) Gallagher, P. K. *Thermochim. Acta* **1978**, *26*, 175.
(14) Gallagher, P. K. *Thermochim Acta* **1984**, *82*, 325.

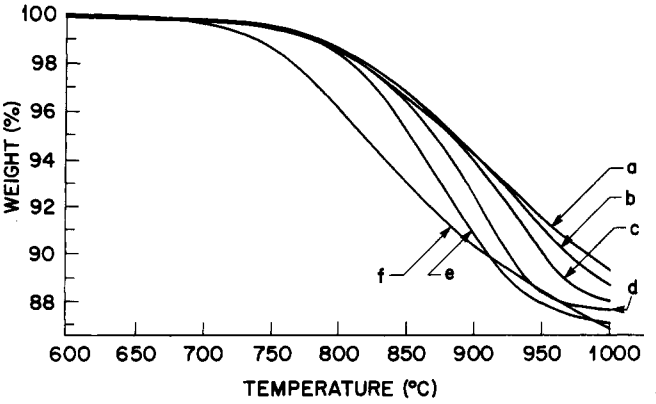

Figure 5. TG curves for the 700 °C calcine, 2 °C min^{-1}: (a) 30.007 mg in O_2, (b) 30.191 mg in air, (c) 29.822 mg in 5.09% O_2, (d) 30.163 mg in 1.03% O_2, (e) 29.570 mg in 0.20% O_2, (f) 28.774 mg in $\sim$50 ppm O_2.

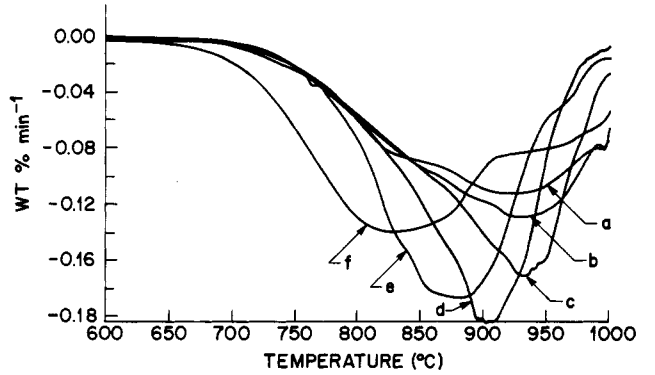

Figure 6. DTG curves for the 700 °C calcine, 2 °C min^{-1}: (a) 30.007 mg in O_2, (b) 30.191 mg in air, (c) 29.822 mg in 5.09% O_2, (d) 30.163 mg in 1.03% O_2, (e) 29.570 mg in 0.20% O_2, (f) 28.774 mg in $\sim$50 ppm O_2.

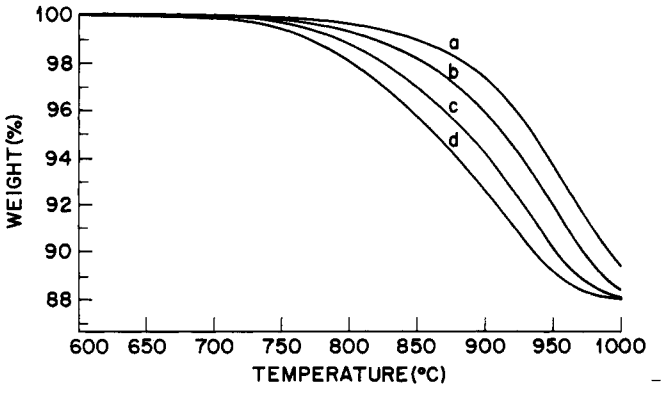

Figure 7. TG curves for the 700 °C calcine, 5.09% O_2 in N_2: (a) 29.921 mg, 10 °C min^{-1}; (b) 29.516 mg, 5 °C min^{-1}; (c) 29.822 mg, 2 °C min^{-1}; (d) 29.796 mg, 1 °C min^{-1}.

Powder X-ray diffraction was performed by using the Philips automated diffractometer with Cu Kα radiation. The patterns obtained for the as-prepared oxalate and for powder after calcination in O_2 at 700 °C for 30 min are given in Figure 4. The surface area of the calcined material was 6.85 $m^2\ g^{-1}$. An average particle size of 0.14 μm is estimated based upon the approximation of spherical particles having a density of 6.3 g cm^{-3}. The X-ray diffraction pattern in Figure 4b is identical, except for its broader lines, with that of the mixture of $BaCO_3$, CuO, and Y_2O_3 used in the traditional ceramic preparation.

Kinetic Study. Because the particle size, chemical composition, and defect structure are most likely quite different for the materials at advanced stages in Figure 1, a more reliable test of the influence of P_{O_2} on the final stage of decomposition, eq 1, is to start at the onset of that final stage with a material having the same thermal history. This is true for the data subsequently

Table I. Temperatures at Selected Fractions Reacted for Various Heating Rates and Atmospheres

		heating rate, °C min^{-1}							
		10 °C		5 °C		2 °C		1 °C	
atm (% O_2)	fraction reacted (α)	*a*	*b*	*a*	*b*	*a*	*b*	*a*	*b*
100	0.1	862.6	868.0	823.5	828.4	788.3	792.6	758.5	762.8
	0.2	907.9	914.2	865.1	871.5	823.4	828.4	791.3	796.4
	0.3	938.8	945.7	897.1	904.7	850.0	857.1	821.8	825.8
	0.4	963.1	970.7	923.5	931.6	875.2	883.5	844.2	849.5
21	0.1	864.9	870.2	827.0	831.9	789.3	793.6	768.1	772.1
	0.2	907.8	913.6	868.5	874.4	824.4	830.8	800.2	805.3
	0.3	935.3	941.5	897.3	904.1	851.6	858.3	825.2	831.5
	0.4	955.8	963.0	921.0	922.0	874.7	882.4	847.4	854.8
5	0.1	859.7	864.6	822.5	827.4	789.2	793.5	768.2	772.3
	0.2	898.1	903.2	862.1	867.7	825.4	830.9	802.4	807.7
	0.3	920.8	926.0	886.6	893.4	851.8	858.2	827.8	834.2
	0.4	937.6	942.9	908.5	914.8	874.1	876.9	849.8	857.1
1	0.1	854.8	858.7	823.1	827.7	787.1	791.4	759.8	763.8
	0.2	883.9	888.2	857.2	861.8	820.9	825.9	793.3	798.3
	0.3	902.2	906.6	877.2	881.9	844.4	849.7	817.1	823.0
	0.4	916.0	920.9	892.1	897.0	862.1	863.0	837.8	843.6
0.2	0.1	845.3	848.3	811.8	816.0	781.9	786.0	753.4	757.6
	0.2	873.6	877.7	840.5	844.4	811.3	815.6	785.4	789.4
	0.3	891.4	895.9	857.8	861.3	829.6	834.3	806.0	810.9
	0.4	905.6	910.6	872.4	876.7	844.1	849.9	821.8	827.2
0.005	0.1	819.0	823.5	775.2	780.9	738.7	742.5	732.2	736.4
	0.2	853.8	858.5	807.1	812.3	767.7	772.2	762.0	766.4
	0.3	875.0	880.3	826.9	833.3	788.7	794.1	782.9	788.1
	0.4	892.3	898.2	844.2	852.4	807.0	813.8	800.2	806.5

[a] Based on an end product of $Ba_2YCu_3O_{6.5}$. [b] Based on an end product of $Ba_2YCu_3O_{6.0}$.

Table II. Activation Energies (kcal mol^{-1}) Calculated from Kinetic Studies at Various P_{O_2}

fraction reacted	% O_2					
(α)	100	20.9	5.09	1.03	0.20	0.005
0.1	52.3	55.4	59.0	56.6	59.0	52.8
0.2	49.8	53.5	60.6	62.8	64.4	52.7
0.3	51.4	55.0	65.6	70.2	68.9	54.6
0.4	52.8	58.4	71.4	77.6	72.2	57.2

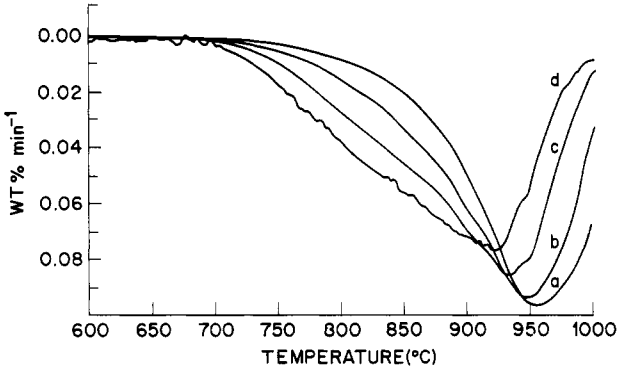

Figure 8. DTG curves for calcine, 5.09% O_2 in N_2: (a) 29.921 mg, 10 °C min^{-1}; (b) 29.516 mg, 5 °C min^{-1}; (c) 29.822 mg, 2 °C min^{-1}; (d) 29.796 mg, 1 °C min^{-1}.

presented in Figures 5–8 and Tables I and II, which are all derived from the single calcine represented by Figure 4b. About 29.5 ± 1 mg samples were heated in Pt pans using a Perkin-Elmer System 7 standard TG furnace arrangement. Heating rates of 10, 5, 2, and 1 °C min^{-1} were used in flowing atmospheres (100 mL min^{-1}) of 100%, 21%, 5.1%, 1.0%, 0.20%, and 0.005% oxygen in nitrogen. The latter value represents the concentration in the exhaust gas from the thermal balance as measured by a Systeck oxygen analyzer. The input was nitrogen with <10 ppm oxygen; however, leaks and outgassing of the apparatus significantly raised the oxygen content.

The sample temperature was calibrated using the Curie temperatures of iron as 780 °C.[9,15] The resulting correction factors

(15) Norem, S. D.; O'Neill, M. J.; Gray, A. P. *Thermochim. Acta* **1970**, *1*, 29.

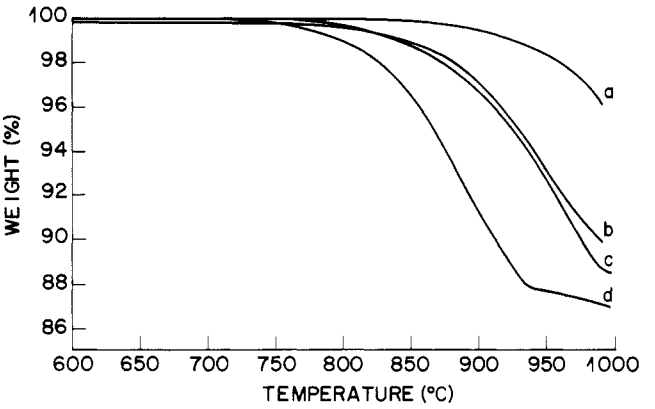

Figure 9. TG curves for conventional mixed $BaCO_3$, Y_2O_3, and CuO powders, 10 °C min^{-1}: (a) 136.458 mg, 0.6 m^2 g^{-1} O_2; (b) 110.690 mg, 0.6 m^2 g^{-1}, ~50 ppm O_2; (c) 49.361 mg, 4.78 m^2 g^{-1} O_2; (d) 54.836 mg, 4.78 m^2 g^{-1}, ~50 ppm O_2.

+7.5, +1.1, −5.4, and −5.6 °C at heating rates 10, 5, 2, and 1 °C min^{-1}, respectively, have been applied prior to analysis of the kinetic data. These corrections are significant, as can be seen from the spread of over 13 °C for the relatively modest variations in heating rate.

The temperature was programmed to rise rapidly (100 °C/min) to 600 °C, hold for 10 min to drive off adsorbed gases, and then heat at the desired rate to 1000 °C. The data collection was started as the sample was heated beyond the isothermal hold period.

A series of TG and DTG curves at a constant heating rate, 2 °C min^{-1}, but different P_{O_2} is shown in Figures 5 and 6, respectively. A similar series of curves at constant P_{O_2}, 5.09% O_2 in N_2, and varying heating rates is presented in Figures 7 and 8. These curves are uncorrected for temperature; however, all values were corrected prior to use in the numerical analysis. Similarly, the weight is corrected for buoyancy and aerodynamic forces by subtraction of a blank run made under identical conditions prior to kinetic analysis. The theoretical weight changes associated with eq 1 are 10.7, 11.8, and 12.9 wt % loss for x = 7.0, 6.5, and 6.0, respectively. The corrected weight percent loss at 1000 °C in Figure 5 ranges from 10.7 in O_2 to 13.4 in N_2, while those in Figure 7 range from 10.8 at 10 °C min^{-1} to 12.2 at 1 °C min^{-1}. For comparison, Figure 9 presents uncorrected TG curves at 10 °C min^{-1} in oxygen and nitrogen for two conventional mixtures,

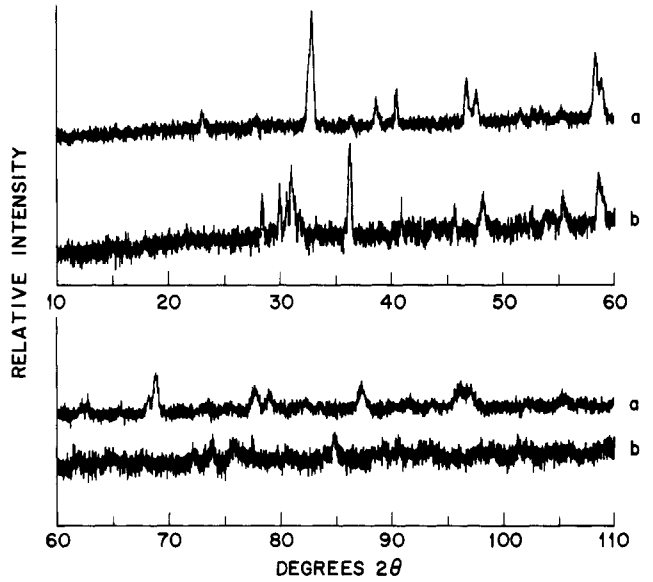

Figure 10. X-ray diffraction for the 700 °C calcine after TG, Cu Kα radiation. (a, top) After 10 °C min^{-1} to 1000 °C in O_2. (b, bottom) After 10 °C min^{-1} to 1000 °C in ~50 ppm O_2.

barium carbonate and the oxides of copper and ytrium. These mixtures have surface areas of 4.78 and 0.6 m^2 g^{-1}.

The Ozawa[16] method of kinetic analysis was applied to the TG data. In this method, the temperatures associated with a particular fraction reacted, α, are determined at different heating rates. A plot of log heating rate versus reciprocal temperature will have a slope proportional to the activation energy, E. This method is applicable to any value of α, but since the product compound will lose oxygen in low P_{O_2} above about 800 °C, the analysis for the decomposition of the carbonate was done for $\alpha \leq 0.4$. Table I presents the corrected temperatures used in analysis. Because of the variation of oxygen content with P_{O_2} and temperature, the value of α is uncertain and the values are tabulated for the two relevant extremes of x. Attributing all of the weight loss to CO_2 would correspond to columns marked by a, while the columns marked by b correspond to an additional loss oxygen to the approximate lower limit of stability of the structure. Under none of the experimental conditions in Table I would the equilibrium value of x exceed 6.5, and if the value drops below 6.0, then the reaction is not that represented by eq 1.

The X-ray diffraction data presented in Figure 10 for the residues of the TG samples heated in oxygen and nitrogen (see Figure 1) clearly indicate that any $Ba_2YCu_3O_x$ formed initially decomposes before 1000 °C in nitrogen. The pattern in Figure 10a for the sample heated in oxygen is that of the orthorhombic structure for $Ba_2YCu_3O_x$, indicating that the specimen took up substantial oxygen during cooling. The sample heated in nitrogen, Figure 10b, however, was unable to do so, and the patterns associated with the decomposition, BaY_2CuO_5, Cu_2O, etc., are evident.

Two series of kinetic plots are shown in Figures 11 and 12 for the data taken in atmospheres of 100% and 1% oxygen in nitrogen, respectively. The lines represent least-squares fits to the data points. There is very little effect on the slope by the choice of end composition, i.e., columns marked by a or b in Table I. The values of the activation energy given in Table II correspond to the average for each pair. The mean difference between the values for a pair was <1 kcal mol^{-1}.

Discussion

From the weight loss data in Figure 1, it is concluded that the starting collective mixed oxalate is $Ba_4Y_2Cu_6(C_2O_4)_{13}\cdot 20H_2O$. The complex X-ray diffraction pattern in Figure 4a would not indicate a single solid solution of the oxalates. A loss of 20 H_2O corresponds to 86.4 wt %

(16) Ozawa, T. *Bull. Chem. Soc. Jpn.* **1965**, *38*, 1881.

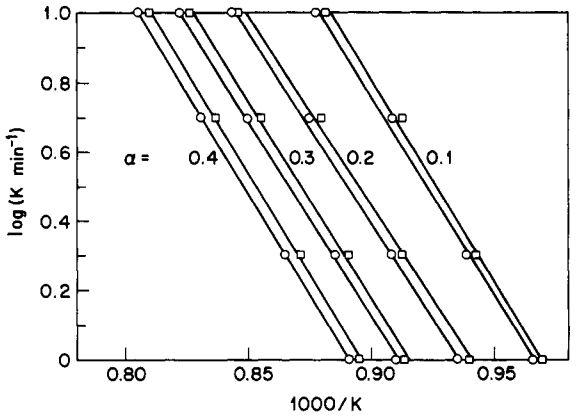

Figure 11. Ozawa plots for calcine, O_2. (□) Table I, columns marked *a*; (○) Table I, columns marked *b*.

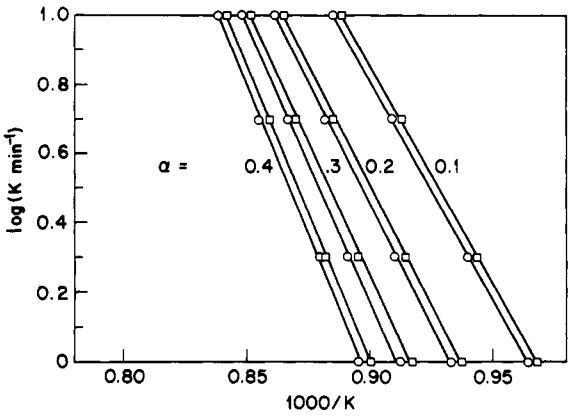

Figure 12. Ozawa plots for calcine, 1% O_2 in N_2. (□) Assuming $x = 6.5$. (○) Assuming $x = 6.0$.

remaining, subsequent decomposition of the ytrium and copper oxalates to their oxides would yield 65.2 wt %, the decomposition of the barium oxalate to carbonate would give 55.8 wt %, and the final decomposition to form $Ba_2YCu_3O_6$ at 1000 °C would equal a remaining weight of 49.2 wt %. These final and intermediate weight levels are in excellent agreement with the inflections and plateaus present in the TG curves in Figure 1. Clearly the large heat due to exothermic oxidation for experiments in atmospheres with high oxygen contents, see Figure 2, leads to the virtually simultaneous decomposition of all the oxalates so that a single weight loss occurs for this event in the oxygen traces in Figure 1. The much smaller exotherm in oxygen around 450 °C in Figure 2 may be the oxidative decomposition of a small amount of remaining BaC_2O_4, some crystallization process, or the oxidation of small amounts of a reduced state of copper and/or carbon residue. The separate decomposition of BaC_2O_4 is clearly evident, however, in the curves for nitrogen in Figures 1 and 2 and the vacuum EGA curves in Figure 3. The assignment of the weight loss around 100 °C to water and the assignments at 200–500 °C to oxalate decomposition are substantiated by the EGA data.

In the temperature range 500–800 °C, an intimate finely divided mixture of $BaCO_3$, Y_2O_3, and CuO is formed in oxidizing atmospheres as indicated by the X-ray diffraction pattern in Figure 4b and the prolonged weight plateau at ~55 wt % in Figure 1. The endothermic phase transition in $BaCO_3$ from the α to the β form at about 810 °C is evident in the DTA patterns. The weight loss curve in Figure 1 for nitrogen suggests that there has been significant decomposition of the $BaCO_3$ prior to 850 °C. Some of this greater weight loss in nitrogen might be explained

by the presence of reduced species of copper, e.g., Cu_2O and their subsequent oxidation by CO_2 or traces of oxygen in the atmosphere during the reaction to form $Ba_2YCu_3O_x$.

The effect of heating rate shown in Figures 7 and 8 is as expected. The temperature and intensity at the maximum rate increase as the heating rate increases, but the overall extent of the reaction has decreased at any specific temperature. The general influence of P_{O_2} upon the rate of reaction can be seen in Figures 5 and 6. The extent of the reaction at a temperature has increased with decreasing P_{O_2}. The temperature of the maximum rate shifts to lower temperatures with decreasing P_{O_2} below 5% O_2. The temperature at the maximum rate in Figure 6 has lowered more the 100 °C on going from 5% O_2 to 50 ppm of O_2. As shown, however, by the X-ray diffraction patterns in Figure 10, the end product at the low values of P_{O_2} and high values of temperature has progressed beyond the reaction represented by eq 1.

It was hoped that restricting the kinetic study to values of $\alpha \leq 0.4$ would avoid that conflict. Indeed, as shown in Table I, all the temperatures used in the kinetic analysis at the lowest P_{O_2} are <900 °C. Even in pure oxygen, the maximum temperature used is 963.1 °C.

The very parallel nature of the plots in the Ozawa analysis for each pair of isocompositional lines in Figures 11 and 12 based on different values of x indicates that concern over the differences in end point is not a significant factor in evaluating the activation energy. In oxygen, Figure 11, the slope of the plots does not vary significantly with α. This is not true, however, in Figure 12 for the data taken in 1% oxygen.

There are potential effects of several transformations on the rate of reaction. The temperature is high enough that the product phase should have had tetragonal symmetry under all conditions. There is, however, a metallic to semiconducting transition in the electrical conductivity that takes place when the value of x in the product phase drops below ~ 6.25[17] and the α to β first-order phase transformation in crystalline $BaCO_3$ occurs around 810 °C. There do not appear to be any indications in the kinetic data that reflect these changes. It is probably unreasonable to expect a significant "Hedvall effect", i.e., an increase in the rate during a crystalline transformation, in these dynamic experiments. Such effects are usually observed isothermally after repeated scans.[18]

The trends in activation energy, E, can be best seen in Table II. There is a tendency toward increasing the activation energy with increasing extent of reaction that is much more prominent as P_{O_2} is lowered. This trend is also apparent in the data in air by Negishi et al.[12] There is also a clear trend toward higher values of E as the P_{O_2} is reduced at constant α. This latter trend seems to break down at the higher values of α and lower values of P_{O_2} where the oxygen content has probably dropped below 6, and second phases begin to form. The boundary for this change seems to occur as α exceeds about 0.2 in 0.2% oxygen or as oxygen drops below about 0.2% at values of $\alpha \geq 0.2$. The ranges of values in Table II are in good agreement with those observed by Negishi et al. in air.[12]

As predicted, based upon the relative defect concentrations, the extent of the reaction is greater at the same temperature for lower values of P_{O_2}, i.e., a higher concentration of defects. It is interesting that this behavior is contrary to that predicted by the tendency of the activation energy to increase with decreasing P_{O_2}. The result must be an increased preexponential term, if an Arrhenius-like rate law is observed. One could speculate that the presence of Y_2O_3 and CuO effectively catalyze the decomposition of $BaCO_3$ (ref 19) and that there is an induction period that is proportional to the P_{O_2}. Such an induction period may be related to the growth of nuclei to the critical size, where these nuclei are vacancy clusters. Lower P_{O_2} favors vacancy formation and, hence, shortens the induction period. However, because the temperatures to reach an α of 0.1 are very similar at $P_{O_2} \geq 5\%$ in Table I, this explanation is only plausible for low P_{O_2}.

Further examination of Table I indicates that the effect of P_{O_2} tends to be cumulative and thus is most apparent at $\alpha = 0.4$. If the effect is due to enhanced nucleation via vacancy clusters, then it must be a continuous and probably even an acceleratory-type process. This apparent self-catalyzing aspect of the behavior is consistent with the dynamic mode of operation; i.e., as the temperature is constantly increased, so is the vacancy concentration. Perhaps more extensive isothermal kinetic studies could unravel the details of the mechanism.

Conclusions

Precipitation by digestion of carbonates, hydroxides, or oxides in oxalic acid solution produces a high-purity and easily filtered precipitate with little if any compensation required for relative solubilities.

This precipitate can be directly converted to $Ba_2YCu_3O_x$ by calcination. Heating to 300 °C in air or 600 °C in nitrogen will produce an intimate mixture of $BaCO_3$–CuO–Y_2O_3 which will react upon further heating to the desired product. The overall rate of this latter reaction is significantly influenced by the P_{O_2} present during this stage. A lower P_{O_2} favors more reaction for the same heating rate. It is speculated that this enhanced rate is the result of higher concentrations of anion vacancies at the lower values of P_{O_2}.

Registry No. $BaCO_3$, 513-77-9; $CuCO_3$, 1184-64-1; YCO_3, 556-28-5; $Ba_4Y_2Cu_6(C_2O_4)_{13}\cdot 20H_2O$, 123676-73-3; $Ba_2YCu_3O_{6.5}$, 109466-64-0; $Ba_2YCu_3O_6$, 109489-85-2; O_2, 7782-44-7; oxalic acid, 144-62-7.

(17) Grader, G. S.; Gallagher, P. K.; Gyorgy, E. M. *Appl. Phys. Lett.* **1987**, *51*, 1115.
(18) Gallagher, P. K.; Johnson, D. W. *J. Phys. Chem.* **1982**, *86*, 295.
(19) Grader, G. S.; Gallagher, P. K.; Fleming, D. A. *Chem. Mater.*, following paper in this issue.